32. Benders, A.A., Groenen, P.J., Oerlemans, F.T., Veerkamp, J.H., and Wieringa, B.J. 1997, *Clin. Invest.*, 100, 1440.
33. Kaliman, P., Catalucci, D., Lam, J.T., Kondo, R., Gutierrez, J.C., Reddy, S., Palacin, M., Zorzano, A., Chien, K.R., and Ruiz-Lozano, P. 2005, *J. Biol. Chem.*, 280, 8016.
34. Pall, G.S., Johnson, K.J., Smith, G.L. 2003, *Physiol. Genomics*, 13, 139.
35. O'Cochlain, D.F., Perez-Terzic, C., Reyes, S., Kane, G.C., Behfar, A., Hodgson, D.M., Strommen, J.A., Liu, X.K., van den Broek, W., Wansink, D.G., Wieringa, B., and Terzic, A. 2004, *Hum. Mol. Genet.*, 13, 2505.
36. Mankodi, A., Logigian, E., Callahan, L., McClain, C., White, R., Henderson, D., Krym, M., and Thornton, C.A. 2000, *Science*, 289, 1769.
37. Seznec, H., Agbulut, O., Sergeant, N., Savouret, C., Ghestem, A., Tabti, N., Willer, J.C., Ourth, L., Duros, C., Brisson, E., Fouquet, C., Butler-Browne, G., Delacourte, A., Junien, C., and Gourdon, G. 2001, *Hum. Mol. Genet.*, 10, 2717.
38. Furling, D., Lemieux, D., Taneja, K., and Puymirat, J. 2001, *Neuromuscul. Disord.*, 11, 728.
39. Sabourin, L.A., Tamai, K., Narang, M.A., and Korneluk, R.G. 1997, *J. Biol. Chem.*, 272, 29626.
40. Usuki, F., Ishiura, S., Saitoh, N., Sasagawa, N., Sorimachi, H., Kuzume, H., Maruyama, K., Terao, T., and Suzuki, K. 1997, *Neuroreport.*, 8, 3749.
41. Amack, J.D., and Mahadevan, M.S. 2001, *Hum. Mol. Genet.*, 10, 1879.
42. Amack, J.D., Reagan, S.R., and Mahadevan, M.S. 2002, *J. Cell Biol.*, 159, 419.
43. Usuki, F., and Ishiura, S. 1998, *Neuroreport.*, 9, 2291.
44. Takeshita, Y., Sasagawa, N.., Usuki, F. et al. 2003, *Basic Appl. Myol.*, 13, 305.
45. Timchenko, L.T., Miller, J.W., Timchenko, N.A., DeVore, D.R., Datar, K.V., Lin, L., Roberts, R., Caskey, C.T., and Swanson, M.S. 1996, *Nucleic Acids Res.*, 24, 4407.
46. Timchenko, N.A., Patel, R., Iakova, P., Cai, Z.J., Quan, L., and Timchenko, L.T. 2004, *J. Biol. Chem.*, 279, 13129.
47. Ho, T.H., Bundman, D., Armstrong, D.L., and Cooper, T.A. 2005, *Hum. Mol. Genet.*, 14, 1539.
48. Michalowski, S., Miller, J.W., Urbinati, C.R., Paliouras, M., Swanson, M.S., and Griffith, J. 1999, *Nucleic Acids Res.*, 27, 3534.
49. Takahashi, N., Sasagawa, N., Suzuki, K., and Ishiura, S. 2000, *Biochem. Biophys. Res. Commun.* 277, 518.
50. Roberts, R., Timchenko, N.A., Miller, J.W., Reddy, S., Caskey, C.T., Swanson, M.S., and Timchenko, L.T. 1997, *Proc. Natl. Acad. Sci. USA*, 94, 13221.
51. Miller, J.W., Urbinati, C.R., Teng-Umnuay, P., Stenberg, M.G., Byrne, B.J., Thornton, C.A., and Swanson, M.S. 2000, *EMBO J.*, 19, 4439.
52. Begemann, G., Paricio, N., Artero, R., Kiss, I., Perez-Alonso, M., and Mlodzik, M. 1997, *Development*, 124, 4321.
53. Kino, Y., Mori, D., Oma, Y., Takeshita, Y., Sasagawa, N., and Ishiura, S. 2004, *Hum. Mol. Genet.*, 13, 495.
54. Kanadia, R.N, Johnstone, K.A., Mankodi, A., Lungu, C., Thornton, C.A., Esson, D., Timmers, A.M., Hauswirth, W.W., Swanson, M.S. 2003, *Science*, 302, 1978.
55. Fardaei, M., Larkin, K., Brook, J.D., and Hamshere, M.G. 2001, *Nucleic Acids Res.*, 29, 2766.

56. Fardaei, M., Rogers, M.T., Thorpe, H.M., Larkin, K., Hamshere, M.G., Harper, P.S., and Brook, J.D. 2002, *Hum. Mol. Genet.*, 11, 805.
57. Ho, T.H., Savkur, R.S., Poulos, M.G., Mancini, M.A., Swanson, M.S., and Cooper, T.A. 2005, *J. Cell Sci.*, 118, 2923.
58. Philips, A.V., Timchenko, L.T., and Cooper, T.A. 1998, *Science*, 280, 737.
59. Savkur, R.S., Philips, A.V., Cooper, T.A. 2001, *Nat. Genet.*, 29, 40.
60. Mankodi, A., Takahashi, M.P., Jiang, H., Beck, C.L., Bowers, W.J., Moxley, R.T., Cannon, S.C., and Thornton, C.A. 2002, *Mol. Cell*, 10, 35.
61. Kimura, T., Nakamori, M., Lueck, J.D., Pouliquin, P., Aoike, F., Fujimura, H., Dirksen, R.T., Takahashi, M.P., Dulhunty, A.F., and Sakoda, S. 2005, *Hum. Mol. Genet.*, 14, 2189.
62. Charlet, B.N., Savkur, R.S., Singh, G., Philips, A.V., Grice, E.A., and Cooper, T.A. 2002, *Mol. Cell*, 10, 45.
63. Buj-Bello, A., Furling, D., Tronchere, H., Laporte, J., Lerouge, T., Butler-Browne, G.S., and Mandel, J.L. 2002, *Hum. Mol. Genet.*, 11, 2297.
64. Sergeant, N., Sablonniere, B., Schraen-Maschke, S., Ghestem, A., Maurage, C.A., Wattez, A., Vermersch, P., and Delacourte, A. 2001, *Hum. Mol. Genet.*, 10, 2143.
65. Jiang, H., Mankodi, A., Swanson, M.S., Moxley, R.T., and Thornton, C.A. 2004, *Hum. Mol. Genet.*, 13, 3079.

Acta Myologica • 2005; XXIV: p. 74-77

Regulation of splicing by MBNL and CELF family of RNA-binding protein

S. Ishiura, Y. Kino, Y. Nezu, H. Onishi, E. Ohno, and N. Sasagawa

Department of Life Sciences, Graduate School of Arts and Sciences, The University of Tokyo, 3-8-1 Komaba, Meguro-ku, Tokyo, Japan 153-8902

Myotonic Dystrophy (DM), the most common form of adult-onset muscular dystrophy, comprises at least 2 subtypes, DM1 and DM2. DM1 is caused by the expansion of a CTG repeat located in the 3' untranslated region of the DM protein kinase (*DMPK*) gene. Recently, the expansion of a CCTG tetranucleotide repeat located in the first intron of the *ZNF9* gene was identified as the mutation responsible for DM2. Since both DM1 and DM2 are caused by the expansion of repetitive sequences, some common factors that interact with these sequences might be involved in the pathogenesis of DM. MBNL1 is a candidate for such factors and is thought to be sequestered by the expanded forms of DM transcripts.

Key words: myotonic dystrophy, RNA repeat, MBNL1

Myotonic dystrophy is the most common form of adult-onset muscular dystrophy [1]. It is inherited by autosomal dominant fashion. Myotonic dystrophy causes a consistent constellation of unrelated clinical features, including myotonia, cardiac conduction defects, cataracts, and specific set of endocrine changes, and so on. The underlying genetic mutation causing myotonic dystrophy is unstable expanded CTG repeat in the 3'-untranslated region of a gene on chromosome 19 encoding a DM protein kinase (DMPK) of unknown function [2]. The mutation is transcribed into RNA but not translated into protein. Recently, myotonic dystrophy type 2 (DM2) was found to be caused by a CCTG tetranucleotide expansion in intron 1 of the Zn-finger protein ZNF-9 gene on chromosome 3 [3]. DM2 is also caused by a transcribed but untranslated repeat expansion. Although DM2 is generally a milder disease than DM1, the DM2 CCTG expansions is much larger than DM1 CTG expansions.

Reddy et al. showed that DMPK knockout mice did not fully recapitulate DM. This means that loss of DMPK function is not the main cause of DM [4]. RNA inclusions of CUG/CCUG repeats are observed as foci in the nuclei of DM patients. Transgenic mice expressing CUG repeats under the skeletal muscle actin promoter showed myotonia and abnormal muscle histology [5]. In this case, the severity of phenotype was correlated with the expression level of CUG repeat RNA. These results suggest that abnormality in RNA metabolism is involved in DM [1].

The clinical features common to both DM1 and DM2 may be caused by a gain-of-function RNA mechanism in which the CUG and CCUG repeats alter cellular function by sequestering repeat RNA-binding proteins.

Two families of RNA-binding proteins

Two families of RNA repeat-binding proteins have been implicated in DM pathogenesis: CELF (CUG-BP1 and ETR-3-like factors) and MBNL(muscleblind-like) proteins. Six CELF genes have been identified in human genome and they have been shown to be involved in alternative splicing [6]. Among these, CUG-BP1 regulates alternative splicing of cardiac troponin T (cTnT), insulin receptor (IR) and chloride channel 1 (ClC-1) that are misregulated in DM muscle [7,8]. MBNL is a homologue of *Drosophila* muscleblind which is involved in the differentiation of muscle and photoreceptor [9]. Three genes (*MBNL1, 2* and *3*) are identified in humans. A mouse knockout reproduced myotonia and cataract, and misregulation of splicing was observed [10].

We investigated the in vivo binding-sequence specificity of these proteins using a yeast 3 hybrid system [11,12]. In this assay, the association of

Address for correspondence: correspondence should be addressed to Dr. S.Ishiura. Department of Life Sciences, Graduate School of Arts and Sciences, The University of Tokyo, 3-8-1 Komaba, Meguro-ku, Tokyo, Japan 153-8902

an RNA-binding protein Y with its cognate RNA X binding site leads to the transcriptional activation of a reporter gene, such as HIS3 and β-galactosidase, in yeast. We generated a variety of repetitive RNA sequences and examined them.

The results are shown in Table 1. CUG-BP1 (this protein is first identified as a CUG triplet repeat-binding protein) strongly interacted with UG dinucleotide repeat [11]. Neither PKR (protein kinase R), a double stranded nucleotide-binding protein, nor CUG-BP1 interacted strongly with CUG/CCUG repeats. By contrast, MBNL1 showed apparent interactions with both CUG and CCUG repeats.

Table 1. RNA-binding specificity of candidate proteins.

Repeat	CUG-BP1	MBNL1	PKR
UG24	+++++	-	-
CA24	-	-	-
CUG7	-	-	-
CUG16	-	++	-
CUG21	-	+++	-
CUG37	-	++	-
CUG70	-	++	+
CCUG7	+	-	-
CCUG22	-	++++	-
CCUG50	-	+++	-
CAGG22	-	-	-
CAGG50	+	-	-
CGGG20	-	-	-
CCCG21	++	++++	-
UAUG7+CAUA7	-	-	+++++
CAG16+CUG16	-	-	+++++

The transformation of yeast cells and reporter gene assays were performed as previously described (11,12). We classified the binding activity as (+++++), (++++), (+++) and (++), when yeast grown was observed on the plates containing 1, 0.5, 0.1 and 0mM 3-AT, respectively. (+) yeast grew in the absence of 3-AT after more than 1 week, (-) no growth of yeast transformants was observed even after prolonged incubation.

We confirmed these results by surface plasmon resonance technique. Surface Plasmon Resonance (SPR) is a powerful technique to measure biomolecular interactions in real-time in a label free environment. Protein is immobilized to the sensor surface, and the repeat RNA is passed over the surface. Association and dissociation is measured and displayed in a graph called the sensorgram. CUG-BP1 strongly interacted with UG-repeat but not CUG repeat, while MBNL1 interacted with CCUG repeat (data not shown). These results indicate that loss of function of MBNL1, not CUG-BP1, may be important for DM pathogenesis. Sequestration of MBNL1 by the long CUG/CCUG repeat may disrupt normal cellular function of MBNL1, which leads to abnormal phenotype of myotonic dystrophy.

Table 1 also shows that MBNL1 interacted strongly with CCCG, modestly with CUUG and CUG, but not at all with CGGG and so on. On the other hand, PKR strongly interacted with double-stranded RNAs. All these results suggest MBNL1 binds to repeats with incomplete double strand, but not to the complete one. The deduced target sequence of MBNL1 could be CHHG or CHG repeat, where H is the nucleotide other than G. Secondary structure of CHHG repeat can be calculated as a long hairpin with mismatches. Since MBNL1 does not bind to CUG/CAG double strand repeat without mismatch, the presence of mismatch is necessary for the binding of MBNL1 to the target sequences.

To confirm the results of the three-hybrid analyses, we performed gel retardation analysis [12]. First, we fused MBNL1 with glutathione S-transferase (GST) in the N-terminus and a His-tag in the C-terminus. GST-MBNL1 was expressed in e.coli and purified. GST-MBNL1 bound to a ^{32}P-labeled CCUG probe, and supershift was observed when an anti-GST antibody was added. The extent of band shift was reduced by adding non-labeled CCUG RNA. We also examined the dependence of the binding between CCUG repeats and MBNL1 on the repeat length. Free probes of CCUG27 and CCUG35 disappeared at the highest dose of MBNL1. The number of shifted bands represents the variety of RNA-protein complexes, mainly reflecting the number of proteins binding to a single probe.

Structure of MBNL1 and homologues

MBNL1 has at least nine splice variants. MBNL1 has four Zn finger motifs at the N-terminal half of the molecule, which may be involved in the RNA-binding. There is a nuclear localization signal at the C-terminus. Some of the isoforms of MBNL1 was localized at the nucleus. The others were in the cytosol. Therefore, MBNL1 might have many cellular functions. Furthermore, not only MBNL1 but also MBNL2 and 3 are reported to be colocalized with RNA foci of

CUG/CCUG repeats. We have determined the binding specificity of these MBNL families to various RNA repeats. MBNL2 and MBNL3 had almost similar specificity to MBNL1 (data not shown). These MBNL isoforms also showed different localization. Therefore we have to be careful for analyzing the data, because three MBNL proteins have many isoforms and these isoforms may have diverse functions in various tissues.

Regulation of alternative splicing by RNA repeat-binding proteins

Myotonic dystrophy is an example of a disease that alters the function of RNA-binding proteins to cause misregulated alternative splicing [1]. Many misregulated alternative splicing events have been demonstrated for eight pre mRNAs. In all cases, normal mRNA splice variants are produced, but the normal developmental splicing pattern is disrupted, resulting in the expression of fetal protein isoforms.

The insulin resistance and myotonia observed in DM1 correlate with the disruption of splicing of targets, IR and ClC-1. The counter regulation of mRNA splicing by the two proteins, CUG-BP1 and MBNL1 is demonstrated [9]. When cTNT mini-gene was expressed with CUG-BP1, a fetal isoform including exon 5 was predominantly expressed, while coexpression with MBNL1 suppressed the formation of the fetal isoform. In the case of insulin receptor minigene, MBNL1 enhanced the formation of long form with exon 11, while CUG-BP1 was not. These results suggest that these two RNA-binding proteins counteracted in vivo.

However, in the case of alpha-actinin, MBNL1 may not always act antagonistically against CUG-BP1s. Alpha-actinin has two exons, nonmuscle type and skeletal muscle type. These are exclusively expressed in vivo. However, in our assay system, MBNL1 does not act antagonistically against CUG-BP1. Both enhanced the production of skipped type (Fig.1). These data also predict that change in expression of these alternative splicing regulators would result in the splicing alterations that have been shown to be characteristic of the myotonic dystrophy. However, all targets of these proteins have never been clarified. In addition, these regulators appear to express independently.

There have been many reports that excess oxidative stress occurs in the muscle with expanded CTG repeats [13-15]. The stress accelerates an apoptotic process, leading to cell death. The increase in oxidative stress in response to expended RNA repeats is likely to involve yet unidentified signaling event that remain to be determined. Misregulation of splicing may also be evoked by the cellular signaling processes.

Acknowledgments

This work was supported in part by grants (to S.I.) from the Ministry of Health, Labor and Welfare, Japan, and the Ministry of Education, Science, Sports and Cuture, Japan.

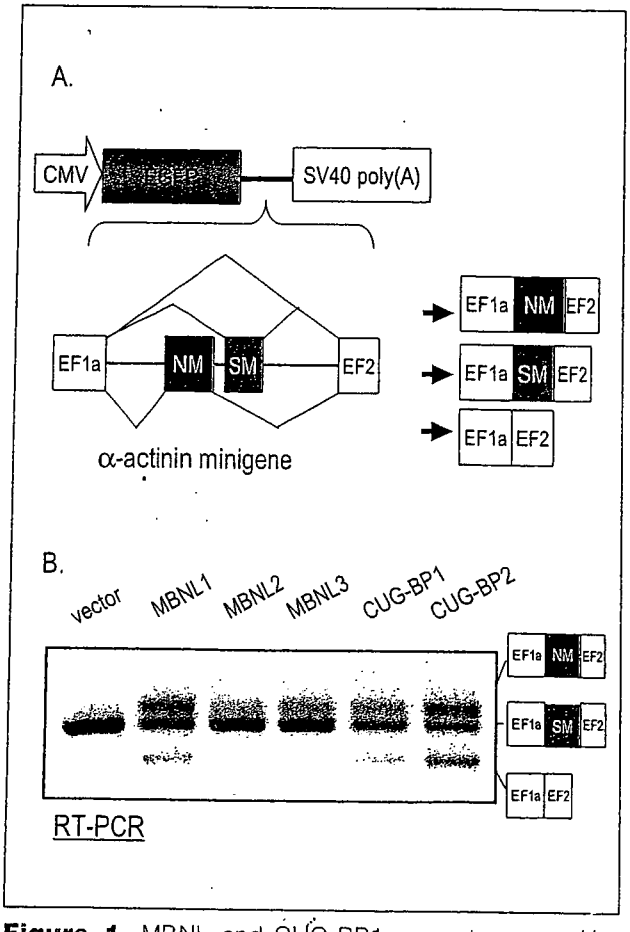

Figure 1. MBNL and CUG-BP1 promote exon skipping.

A. The α-actinin minigene contains two exons (nonmuscle type NM and smooth muscle type SM) flanked by EF1a and EF2 exons.

B. COS cells were cotransfected with the minigene and each of RNA-binding protein expression plasmid. Exon inclusion was assayed by RT-PCR.

References

1. Ranum LPW, Day JW. Myotonic dystrophy:RNA pathogenesis comes into focus. Am J Hum Genet 2004;74:793-804.
2. Sasagawa N, Ishiura S. Myotonic dystrophy protein kinase. Wiley Encyclopedia Mol Med 2002;5:2203-5.
3. Day JW, Ricker K, Jacobson JF, et al. Myotonic dystrophy type 2:molecular, diagnostic and clinical spectrum. Neurology 2003;60:657-64.
4. Reddy S, Smith DB, Rich MM, et al. Mice lacking the myotonic dystrophy protein kinase develop a late onset progressive myopathy. Nat Genet 1996;13:325-35.
5. Ladd AN, Nguyen NH, Malhotra K, Cooper TA. CELF6, a member of the CELF family of RNA-binding proteins, regulates muscle-specific enhancer-dependent alternative splicing. J Biol Chem 2004;279:17756-64.
6. Mankodi A, Logigian E, Callahan L, et al. Myotonic dystrophy in transgenic mice expressing an enpanded CUG repeat. Science 2000;289:1769-73.
7. Timchenko LT, Timchenko NA, Caskey CT, Roberts R. Novel proteins with binding specificity for DNA CTG repeats and RNA CUG repeats: implication for myotonic dystrophy. Hum Mol Genet 1996;5:1115-21.
8. Ho TH, Bundman D, Armstrong DL, Cooper TA. Transgenic mice expressing CUG-BP11 reproduce splicing mis-regulation observed in myotonic dystrophy. Hum Mol Genet 2005;14:1539-47.
9. Ho TH, Charet-B N, Poulos MG, et al. Muscleblind proteins regulate alternative splicing. EMBO J 2004;23:3103-12.
10. Kanadia RN, Johnstone KA, Mankodi A, et al. A muscleblind knockout model for myotonic dystrophy. Science 2003;302:1978-80.
11. Takahashi N, Sasagawa N, Suzuki K, Ishiura S. The CUG-binding protein (CUG-BP1) binds specifically to UG dinucleotide repeats in a yeast three-hybrid system. Biochem Biophys Res Commun 2000;277:518-23.
12. Kino Y, Oma Y, Sasagawa N, Ishiura S. Muscleblind protein, MBNL1/EXP, binds specifically to CHHG repeats. Human Mol Genet 2004;13:495-507.
13. Usuki F, Takahashi N, Sasagawa N, Ishiura S. Differential signaling pathways following oxidative stress in mutant myotonin protein kinase cDNA transfected C2C12 cell lines. Biochem Biophys Res Commun 2000;267:739-43.
14. Usuki F, Yasutake A, Umehara F, et al. In vivo protection of a water-soluble derivative of vitamin E, Trolox, against methylmercury-intoxication in the rat. Neurosci Lett 2001;304:199-203.
15. Takeshita Y, Sasagawa N, Usuki F, Ishiura S. Decreased expression of alpha-B-crystallin in C2C12 cells that express human DMPK/160CTG repeats. Basic Appl Myol 2003;13:305-8.

J Neuropathol Exp Neurol

Vol. 64, No. 6
June 2005
pp. 513–522

ORIGINAL ARTICLE

Autophagic Vacuoles with Sarcolemmal Features Delineate Danon Disease and Related Myopathies

Kazuma Sugie, MD, PhD, Satoru Noguchi, PhD, Yoshimichi Kozuka, PhD, Eri Arikawa-Hirasawa, MD, PhD, Mikihito Tanaka, PhD, Chuanzhu Yan, MD, Paul Saftig, PhD, Kurt von Figura, PhD, Michio Hirano, MD, Satoshi Ueno, MD, PhD, Ikuya Nonaka, MD, PhD, and Ichizo Nishino, MD, PhD

Abstract

Among the autophagic vacuolar myopathies (AVMs), a subgroup is characterized pathologically by unusual autophagic vacuoles with sarcolemmal features (AVSF) and includes Danon disease and X-linked myopathy with excessive autophagy. The diagnostic importance and detailed morphologic features of AVSF in different AVMs have not been well established, and the mechanism of AVSF formation is not known. To address these issues, we have performed detailed histologic studies of myopathies with AVSF and other AVMs. In Danon disease and related AVMs, at the light microscopic level, autophagic vacuoles appeared to be accumulations of lysosomes, which, by electron microscopy consisted of clusters of autophagic vacuoles, indicative of autolysosomes. Some autolysosomes were surrounded by membranes with sarcolemmal proteins, acetylcholinesterase activity, and basal lamina. In Danon disease, the number of fibers with AVSF increased linearly with age while the number with autolysosomal accumulations decreased slightly, suggesting that AVSF are produced secondarily in response to autolysosomes. Most of the AVSF form enclosed spaces, indicating that the vacuolar membranes may be formed in situ rather than through sarcolemmal indentation. This unique intracytoplasmic membrane structure was not found in other AVMs. In conclusion, AVSF with acetylcholinesterase activity are autolysosomes surrounded by secondarily generated intracytoplasmic sarcolemma-like structure and delineates a subgroup of AVMs.

Key Words: Autophagic vacuole, Autophagy, Danon disease, LAMP-2, Lysosome.

From the Departments of Neuromuscular Research (KS, SN, MT, CY, I Nishino) and Ultrastructural Research (YK), National Institute of Neuroscience, National Hospital for Mental (I Nonaka, I Nishino), Nervous and Muscular Disorders, National Center of Neurology and Psychiatry, Kodaira, Tokyo, Japan; the Department of Neurology (KS, SU), Nara Medical University, Kashihara, Nara, Japan; the Department of Neurology (EA-H), Juntendo University School of Medicine, Tokyo, Japan; the Department of Biochemistry (PS), University of Kiel, Kiel, Germany; Zentrum Biochemie und Moleculare Zellbiologie (PS, KvF), Abteilung Biochemie II, Universität Göttingen, Göttingen, Germany; and the Department of Neurology (MH), Columbia University, New York, New York.

Send correspondence and reprint requests to: Ichizo Nishino, MD, PhD, Department of Neuromuscular Research, National Institute of Neuroscience, National Center of Neurology and Psychiatry (NCNP), 4-1-1 Ogawahigashi-cho, Kodaira, Tokyo 187-8502, Japan; E-mail: nishino@ncnp.go.jp

INTRODUCTION

Danon disease, an X-linked vacuolar cardiomyopathy and myopathy, is caused by primary deficiency of lysosome-associated membrane protein-2 (LAMP-2), a major lysosomal membrane protein (1–4). Muscle biopsies contain small autophagic vacuoles with cytoplasmic debris. The membranes of these vacuoles have structural features of sarcolemma and biochemical activities of acetylcholinesterase (AChE) and nonspecific esterase (NSE) (5). Although some sarcolemmal proteins, including dystrophin, have been detected in vacuolar membranes (3), the presence of other sarcolemmal proteins has not been studied. In addition, the pathomechanism by which LAMP-2 deficiency leads to the formation of these peculiar autophagic vacuoles with sarcolemmal features (AVSFs) is still unknown.

AVSFs are also seen in X-linked myopathy with excessive autophagy (XMEA) (6), infantile autophagic vacuolar myopathy (AVM) (7), and adult-onset AVM with multiorgan involvement (8). XMEA is clinically characterized by a mild pure skeletal myopathy. In contrast, infantile AVM involves both cardiac and skeletal muscles and patients die within several months after birth, whereas adult-onset AVM affects multiple organs including liver, kidney, and skeletal muscles. All of these diseases show multilayered basal lamina and the deposition of C5b-9 over the surface of the muscle fiber; these features are not seen in Danon disease. Nevertheless, these diseases are likely to share a common pathomechanism since they also have AVSF similar to those seen in Danon disease (9).

To delineate subtypes of AVMs and to gain insights into their pathomechanisms, we have performed detailed histologic evaluations of muscle from patients with Danon disease, XMEA, infantile AVM, and adult-onset AVM, and from LAMP-2 deficient mice (10, 11). Moreover, to evaluate the specificity of the AVSF we have also characterized autophagic vacuoles in other lysosomal myopathies, including acid maltase deficiency (AMD), sporadic inclusion body myositis (SIBM), and distal myopathy with rimmed vacuoles (DMRV), which has recently been shown to be the same disease as hereditary inclusion body myopathy (HIBM).

MATERIALS AND METHODS

Patients

We examined skeletal muscles of ten affected men from 8 families with genetically confirmed Danon disease. We also

confirmed this diagnosis by immunohistochemistry to demonstrate absence of LAMP-2 in skeletal muscle. Age at muscle biopsy varied from one year to 29 years, average 15 years ± 9. One patient underwent 2 biopsies from his left biceps brachii muscle at ages one year and from his right quadriceps femoris muscle at age 16 years (12). We also studied muscle from a 2-month-old boy with infantile AVM (7), a 41-year-old man with adult-onset AVM with multiorgan involvement (8), and an 18-year-old man with probable XMEA who showed typical clinicopathologic features of the disease but without a family history of myopathy.

Control specimens were obtained from 10 individuals with morphologically normal muscle. In addition, we also studied muscle from 21 patients with AMD (9 infants, 6 children, and 6 adults), 18 patients with DMRV/HIBM, and 20 patients with SIBM. We confirmed that all DMRV/HIBM patients had mutations in the gene encoding UDP-N-acetylglucosamine 2-epimerase/N-acetylmannosamine kinase (13).

Histochemistry

All biopsy specimens were taken from either the biceps brachii or quadriceps femoris muscle. These tissue samples were frozen in liquid nitrogen-cooled isopentane for histochemistry and immunohistochemistry. Transverse serial frozen sections of 8-μm thickness were stained with hematoxylin and eosin (H&E), modified Gomori trichrome, and a battery of histochemical methods, including AChE and NSE stains.

Immunohistochemistry

We performed indirect immunofluorescence staining on 5-μm serial cryosections of muscle according to previously described methods (14). These sections were incubated at 37°C for 2 hours with primary mouse monoclonal IgG antibodies against AChE, lysosomal membranous proteins: LAMP-1, lysosomal integral membrane protein-1 (LIMP-1), LIMP-2, and 19 primary monoclonal or polyclonal antibodies against various sarcolemmal proteins and extracellular matrix proteins (Tables 1 and 2). We also used antibodies against an intralysosomal protein, cathepsin L, and endosomal proteins, VAMP-7, Rab5, transferrin receptor (TfR), and low-density lipoprotein receptor (LDL-R). These were subsequently incubated at room temperature for 1 hour with a secondary antibody, fluorescein isothiocyanate (FITC)-labeled goat F(ab')2 anti-mouse IgG (Leinco Technology, St. Louis, MO) or anti-rabbit IgG (H&L) (Leinco). For double immunolabeling using mouse monoclonal anti-LIMP-1 and rabbit polyclonal anti-dystrophin antibodies (a generous gift from Dr. Imamura), we used two secondary antibodies: FITC-labeled anti-mouse IgG (Leinco) and rhodamine-labeled anti-rabbit IgG (Leinco). We also have stained serial sections with Alexa 488 conjugated α-bungarotoxin (Molecular Probe, Eugene, OR) and were examined by fluorescence microscopy. Furthermore, in other sections, after incubation with primary antibodies we stained with the avidin-biotin-peroxidase complex method (Vector Laboratories, Burlingame, CA) using another secondary antibody: biotinylated goat anti-mouse IgG (Vector). The reaction was visualized with 3,3'-diaminobenzidine (DAB) as the substrate, yielding a brown reaction product. Normal mouse IgG, diluted to the same concentration as the primary antibodies, was used as a negative control.

To estimate presence of the sarcolemmal proteins in vacuolar membrane, we scored the signal of the antibodies from negative (−) to strong (+++) relative to their immunoreactivity in the sarcolemma. The strong score (+++) indicates that the reactivity level in vacuoles equals that in the sarcolemma. Moreover, we counted the numbers of 1) muscle fibers with intracytoplasmic vacuoles highlighted with dystrophin, and 2) muscle fibers with intracytoplasmic overexpression of LIMP-1, in randomly selected fields of all the patients, and calculated the average percentages of both types of muscle fibers in each patient. Statistical analysis of the correlation between the age of the patients and the numbers of muscle fibers immunoreacting dystrophin or LIMP-1 was performed using linear regression.

Electron Microscopy

For electron microscopy, biopsy specimens were fixed in buffered 2% isotonic glutaraldehyde at pH 7.4, postfixed in osmium tetroxide, and embedded in Epoxy resin. Ultrathin sections were stained with uranyl acetate and lead nitrate, and examined with an H-7000 electron microscope (Hitachi, Tokyo, Japan).

Immunoelectron Microscopy

We performed immunoelectron microscopy by preembedding labeling methods. We used muscle biopsy specimens frozen in liquid nitrogen-cooled isopentane without paraformaldehyde prefixation. The specimens were cut in a cryostat into 10-μm transverse sections without thawing and fixed in chilled 4% paraformaldehyde solution in 0.1M phosphate buffer (pH 7.4) for 10 minutes. The fixed sections were washed 5 times in phosphate-buffered saline (PBS). To eliminate nonspecific reactions, sections were incubated for 30 minutes at room temperature in PBS containing 10% normal goat serum and 1% bovine serum albumin (BSA) with PBS. The sections were then incubated at 4°C overnight with one of the following primary mouse monoclonal IgG antibodies: LIMP-1 and the C-terminus of dystrophin. After washing for 30 minutes in PBS, the sections were incubated at 4°C overnight with a secondary antibody: 10-nm-gold-labeled rat anti-mouse antibody (British Biocell International, Cardiff, UK). Subsequently, the sections were fixed in 0.5% glutaraldehyde and postfixed in osmium, and embedded in Epoxy resin. Ultrathin sections were counterstained with uranyl acetate and lead nitrate.

LAMP-2-Deficient Mice and Pathological Methods

We analyzed tibialis anterior muscle from 2 LAMP-2-deficient mice (10, 11) at ages 4 months and 16 months and age-matched normal mice. Muscle specimens were frozen in liquid nitrogen-cooled isopentane for histochemistry and immunohistochemistry or fixed with glutaraldehyde for electron microscopy. Transverse serial frozen sections of 10-μm thickness were stained with H&E, modified Gomori trichrome,

TABLE 1. Summary of Histochemistry and Immunohistochemistry in Various Myopathies with Autophagic Vacuoles

			Expression on Vacuolar Membrane		
	Manufacturer of Antibody	Dilution	Danon Disease and Related AVMs	Rimmed Vacuolar Myopathies	AMD
Histochemistry					
NSE	–	–	+++	–	–
AChE	–	–	+++	–	–
PAS	–	–	+	–	+++
Acid P	–	–	± to ++	++	++
Immunohistochemistry					
AChE	Chemicon, Temecula, CA	1:2000	+++	–	–
AChR	Molecular Probe, Eugene, OR	1:300	–	–	–
C-terminus of Dystrophin	Novocastra, Newcastle Upon Tyne, UK	1:100	+++	– to +	– to +
Rod domain of Dystrophin	Novocastra	1:50	+++	– to +	– to +
N-terminus of Dystrophin	Novocastra	1:20	+++	– to +	– to +
α-Sarcoglycan	Novocastra	1:100	+++	– to +	– to +
β-Sarcoglycan	Novocastra	1:100	+++	– to +	– to +
γ-Sarcoglycan	Novocastra	1:200	++	– to +	– to +
δ-Sarcoglycan	Novocastra	1:50	+++	– to +	– to +
α-Dystroglycan	Upstate, Lake Placid, NY	1:100	++	– to +	– to +
β-Dystroglycan	Novocastra	1:200	+++	– to +	– to +
Dystrobrevin	RDI, Flanders, NJ	1:100	++	– to +	– to +
Dysferlin	Novocastra	1:50	++	– to +	– to ±
Utrophin	Novocastra	1:50	+	– to ±	–
Caveolin-3	Transduction Labs, Lexington, KY	1:100	++	– to +	– to +
β-Spectrin	Novocastra	1:100	++	– to +	– to +
Laminin α2	Chemicon,	1:5000	++	– to +	– to +
Integrin β1	Genex, Helsinki, Finland	1:100	+++	– to +	– to +
Perlecan	Chemicon	1:100	++	– to +	– to +
Agrin	A generous gift from Dr. Sugiyama (32)	1:100	++	– to +	– to +
Fibronectin	Biomedical Tech., Stoughton, MA	1:1000	++	– to ±	– to ±
Collagen IV	Novocastra	1:1000	– to +	– to ±	– to ±
Collagen VI	ICN, Aurora, OH	1:500	– to +	–	– to ±

Both antibodies against fibronectin and agrin were rabbit polyclonal antibodies. All the other antibodies were mouse monoclonal antibodies. AChR was evaluated by binding to α-bungarotoxin. AMD, acid maltase deficiency; NSE, non-specific esterase; AChE, acetylcholinesterase; PAS, periodic acid Schiff; Acid P, acid phosphatase; AchR, acetylcholine receptor.

and a battery of histochemical methods, and the same immunohistochemical methods described above.

RESULTS

Histochemistry and Immunohistochemistry

By routine histologic studies, the vacuolar membranes in Danon disease, probable XMEA, infantile AVM and adult-onset AVM were essentially identical (Table 1). All muscle samples showed mild to moderate variation in fiber size. There were no necrotic fibers except in muscle from adult-onset AVM, which revealed a few necrotic and regenerating fibers. There were scattered small basophilic granules rather than vacuoles in the muscle fibers in H&E-stained sections (Fig. 1). Histochemistry revealed AChE and NSE activities in the vacuolar membranes and the vacuolar structures of the granules. Immunohistochemistry also confirmed presence of AChE in those vacuoles. However, they did not bind to α-bungarotoxin, indicating the absence of acetylcholine receptors (AChRs) in the vacuolar membranes.

By immunohistochemistry, the AVSF reacted for all the tested sarcolemmal and extracellular matrix proteins in the vacuolar membranes in muscle from patients with Danon disease and related AVMs, although reactivity levels of the proteins were variable (Table 1; Fig. 1). However, only collagens IV and VI showed less intense reactivity in the vacuolar membranes than that in the sarcolemma. Most of the AVSFs were scattered throughout the cytoplasm rather than clustered in the subsarcolemmal region. On serial transverse 5-μm sections, most of the AVSFs formed a closed space and the vacuolar membranes were not connected to the sarcolemma with only a few exceptions (Fig. 1Y). Longitudinal sections demonstrated the oval shape of the AVSF, confirming the closed structure of the vacuoles (Fig. 1Z). Vacuolar membranes connected to the sarcolemma were seen in only 2 patients; both were more than 20 years old.

In muscle from patients with Danon disease, LIMP-1, a lysosomal membrane protein, showed accumulations scattered

TABLE 2. Summary of Lysosomal and Endosomal Proteins for Immunohistochemistry in Danon Disease and Related AVMs

Antigen	Manufacturer	Dilution	Expression in the Muscle Fibers
Lysosomal protein			
LAMP-1	Developmental Studies Hybridoma Bank (DSHB), Iowa City, IA	1:100	++
LAMP-2	DSHB	1:100	–
LIMP-1	DSHB	1:100	+++
LIMP-2	A generous gift from Dr. Tanaka (10)	1:200	+
Cathepsin L	Abcam, Cambridge, UK	1:100	+
Endosomal protein			
Rab5	BD Bioscience, Franklin Lakes, NJ	1:50	+
LDL-R	Progen Biotechnik, Heidelberg, Germany	1:100	+
VAMP-7	A generous gift from Dr. Galli (29)	1:200	++
Transferrin R	Lab Vision, Fremont, CA	1:100	+

Antibody against LIMP-2 was rabbit polyclonal and antibody against LDL-R was chicken polyclonal. All the other antibodies were mouse monoclonal.

throughout the fibers in a distribution identical to that of the small basophilic granules on H&E-stained sections (Fig. 2; Table 2), indicating that most autophagic vacuoles in Danon disease are autolysosomes. These autolysosomal accumulations were surrounded by dystrophin-positive membranes in some fibers but not in others (Fig. 2). LAMP-1 and LIMP-2 showed slightly increased expression in fibers with LIMP-1-positive granules (data not shown). Muscle fibers with dystrophin-positive vacuoles accounted for 0.5% to 14.3%, increasing in proportion with age ($y = 0.016 + 0.40x$, $r = 0.94$; Fig. 3). Muscle fibers with autolysosomal accumulations, both with and without dystrophin-positive vacuolar membranes, accounted for 23.7% to 28.7%, showing a slight tendency to decrease with age ($y = 28.6 - 0.15x$, $r = 0.71$; Fig. 3).

LDL-R, TfR, and Rab5 showed mild upregulation mainly in fibers with autolysosomal accumulations in Danon disease and related AVMs (Table 2). Cathepsin L was expressed weakly, mainly in fibers with autolysosomal accumulations. Only VAMP-7 was strongly expressed, mainly in the non-vacuolated fibers without autolysosomal accumulations.

There were occasional intracytoplasmic vacuoles with sarcolemmal proteins in muscles from patients with other AVMs (i.e. DMRV/HIBM, SIBM, and AMD) but their presence was less consistent than in Danon disease and related AVMs. In addition, they never showed AChE or NSE activity. In DMRV/HIBM and SIBM, fibers with sarcolemmal protein-associated vacuoles accounted for approximately 5% to 15% of fibers with rimmed vacuoles (Fig. 4; Table 1). In AMD, sarcolemmal and extracellular matrix proteins were present in some vacuolar membranes. The frequency of fibers with sarcolemmal proteins-associated vacuoles was less than 5% of vacuolated fibers in infantile AMD, and 10% to 15% of vacuolated fibers in childhood and adult-onset AMD.

Electron Microscopy and Immunoelectron Microscopy

In Danon disease and related AVMs, electron microscopy revealed scattered clusters of autophagic vacuoles containing cytoplasmic debris, electron dense materials, and myeloid bodies. Some of these autophagic vacuoles had basal lamina on the luminal side, while other clusters were not limited by a membrane (Fig. 5).

Immunoelectron microscopy showed many autophagic vacuoles; however technical limitations posed by preparing samples from frozen tissue without prefixation prevented us from clearly defining vacuolar membranes. At higher magnification, dystrophin signals were detected on the cytoplasmic side of the vacuolar membrane and along the periphery of the vacuoles (Fig. 5). In contrast, the LIMP-1 antibody signals were associated with autophagic materials including glycogen particles and cytoplasmic debris within the vacuoles, suggesting that the vacuoles are limited by membranes with sarcolemmal features and contain multiple small autophagic vacuoles derived from autolysosomes.

Muscle Pathology in Mice

Muscles from LAMP-2-deficient mice at both 4 and 18 months of age showed features of AVSFs at both light and electron microscopic levels. There were slight variations in fiber size and small vacuoles with basophilic granules by H&E. The granules contained acid phosphatase-positive material. These AVSFs had AChE and NSE activities similarly to those in Danon disease. The frequency of muscle fibers with the AVSFs decorated by NSE and AChE activities was 0.4% at 4 months and 8% at 16 months (data not shown). On immunohistochemistry, the vacuolar membranes were stained with antibodies against dystrophin and other sarcolemmal proteins as well as extracellular matrix proteins, whereas LAMP-2 was completely absent in the muscle. On electron microscopy, there were scattered intracytoplasmic autophagic vacuoles with glycogen particles and cytoplasmic debris (data not shown).

DISCUSSION

In muscle from patients with Danon disease and related AVMs, the membranes of AVSF showed immunoreactivity for all of the sarcolemmal and extracellular matrix proteins tested. Dystrophin and dystrobrevin are cytoskeletal proteins localized along the cytoplasmic side of the sarcolemma (15). Sarcoglycans and β-dystroglycan are transmembranous proteins and are components of "dystrophin bolts" (16). Utrophin

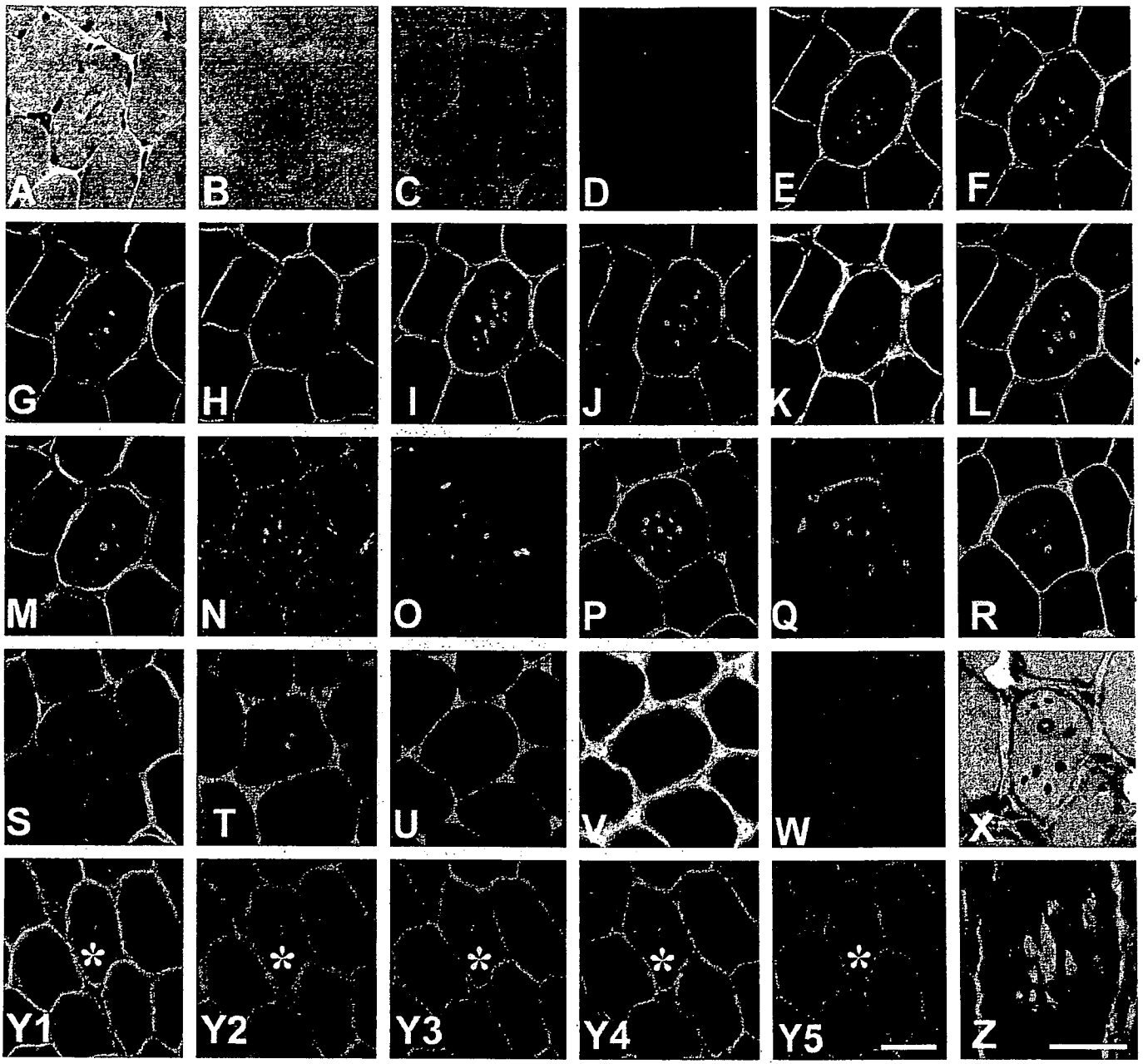

FIGURE 1. Histochemistry and immunohistochemistry. Transverse sections of skeletal muscle biopsies from Danon disease patients. Several fibers contain scattered tiny basophilic intracytoplasmic vacuoles (**A**): H&E. The vacuolar membrane has high nonspecific esterase (**B**) and acetylcholinesterase (**C**) activities. None of the vacuoles bind to α-bungarotoxin (**D**). Sections were stained with antibody against the C-terminus of dystrophin (**E**), the rod domain of dystrophin (**F**), the N-terminus of dystrophin (**G**), laminin α2 (**H**), α-sarcoglycan (**I**), β-sarcoglycan (**J**), γ-sarcoglycan (**K**), δ-sarcoglycan (**L**), dystrobrevin (**M**), α-dystroglycan (**N**), utrophin (**O**), dysferlin (**P**), β-dystroglycan (**Q**), perlecan (**R**), caveolin-3 (**S**), collagen IV (**T**), fibronectin (**U**), collagen VI (**V**), integrin β1 (**W**), and agrin (**X**). The vacuolar membranes were immuno-positive with most of the primary antibodies, although reactivity of these proteins was variable. The results are summarized in Table 1. Transverse 5-μm serial sections (**Y1–Y5**) and longitudinal section (**Z**) of muscle from Danon disease patient showing immunoreaction for dystrophin. Vacuolar membrane in muscle fiber (*) is not connected to the sarcolemma but is closed. Longitudinal section shows that the vacuoles are spherical or oval. (**D–W, Y1–Y5, Z**): FITC-labeled staining; (**X**): DAB staining. (**C–S, U, V, Y1–Y5**): serial sections. Scale bars: (**A–W, Y1–Y5**) = 20 μm; (**Z**) = 30 μm.

is a submembranous protein structurally similar to dystrophin and is widely expressed, albeit at low levels, in the sarcolemma (17). Integrin β1 and α7 are transmembranous proteins and form a complex with each other in the sarcolemma (18). Dysferlin and caveolin-3 are also sarcolemmal proteins and are responsible for limb-girdle muscular dystrophy (LGMD) 2B and LGMD 1C, respectively (19, 20). Extracellular proteins, collagen IV, perlecan, fibronectin, agrin, and laminin, are the

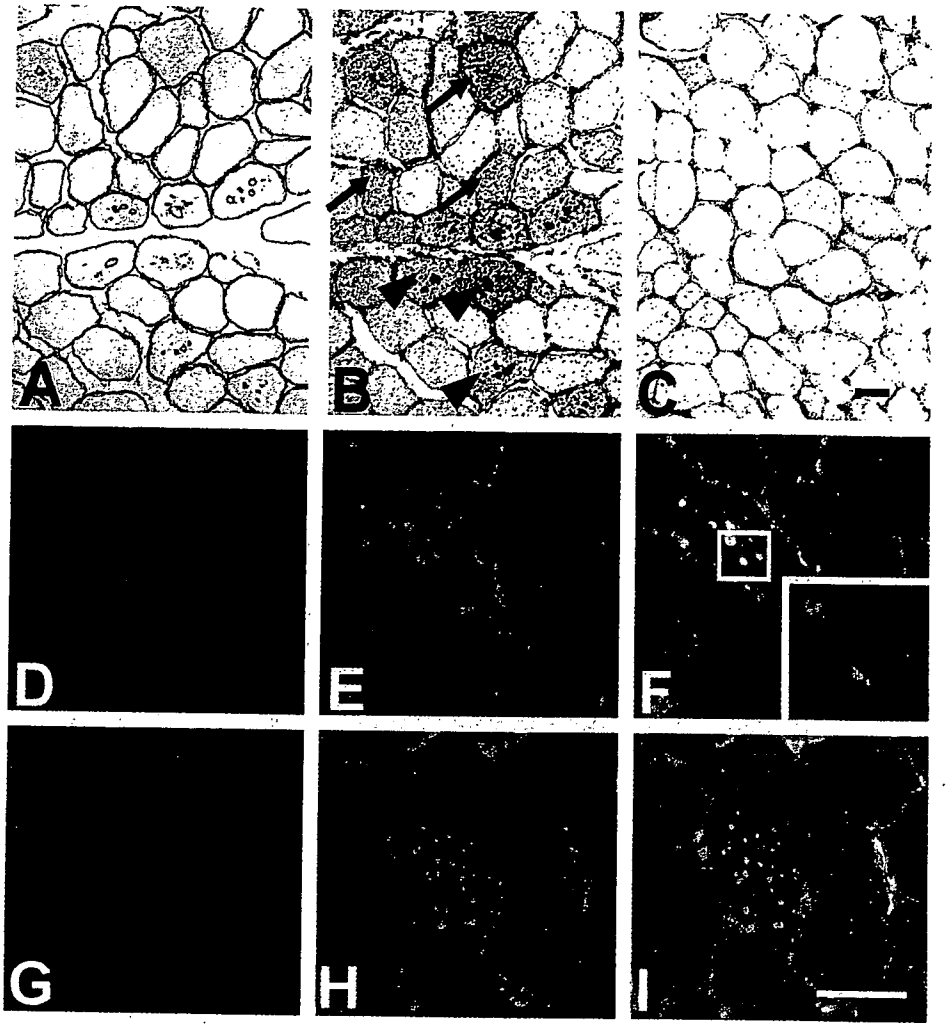

FIGURE 2. Indirect immunohistochemistry. Transverse sections of skeletal muscle stained with DAB for dystrophin (A) and LIMP-1 (B, C). (A, B) Danon disease patient; (C): Normal control. In Danon disease some muscle fibers express both LIMP-1 and dystrophin (arrowheads), whereas some muscle fibers show overexpression of LIMP-1 with absence of dystrophin (arrows). Normal control showed almost no expression of LIMP-1 (C) in muscle fibers. Scale bar = 40 μm. Double immunohistochemistry. Transverse sections of skeletal muscle from Danon disease patient, stained for dystrophin and LIMP-1. LIMP-1 is strongly accumulated inside the muscle fibers (D, G). In some muscle fibers, LIMP-1-positive accumulations are clearly surrounded by dystrophin immunopositive membrane (D–F). These vacuoles are the AVSF. In other muscle fibers, LIMP-1-positive accumulations are not surrounded by dystrophin (G–I). (D, G): dystrophin; (E, H): LIMP-1; (F, I): merged. Scale bar = 30 μm.

main components of the basal lamina. Collagen VI is present in the interstitium but is associated directly with collagen IV (21). We observed very little staining of only collagens IV and VI in vacuolar membranes, indicating that the membranes hardly contain these collagens. Based on our findings, we deduce that the vacuolar membrane of AVSFs in Danon disease and related AVMs have most of the sarcolemmal proteins ranging from cytoplasmic dystrophin to the extracellular laminin.

The vacuolar membranes of AVSF have abundant activities of AChE similar to neuromuscular junctions. Nevertheless, they are distinct from motor endplates because the membranes lacked AChRs. In the early stages of formation of the neuromuscular junction, AChE and AChRs are localized diffusely throughout the sarcolemma. When axon terminals make contact with muscle cells, postjunctional folds are quickly formed. In this process, AChE and AChRs accumulate at junctions and disappear from the extra-junctional sarcolemma (22, 23). These facts support our hypothesis that the vacuoles are intracellular enclosed spaces, because, if AVSF were derived from sarcolemma, then AChE-expressing vacuoles should be located near neuromuscular junctions rather than scattered in the cytoplasm. Furthermore, the presence of AChE without AChRs clearly indicates that the vacuolar membranes are distinct from either junctional or extra-junctional sarcolemma and suggests that they are formed through a unique process.

In the intracellular degradative process called autophagy, "isolation membranes" initially sequesters portions of cytoplasm to be degraded and forms "autophagosomes," which then fuse with lysosomes and become "autolysosomes." The cytoplasm sequestered in autolysosomes is then digested by proteolytic enzymes provided by the lysosomes. Most autophagic vacuoles in Danon disease are autolysosomes rather than autophagosomes, which lack enzymatic activity. These are indicated by the demonstration of many LIMP-1-positive accumulations scattered throughout the fibers (24, 25) and the autophagic nature of the vacuoles on electron microscopy. Actually, small basophilic granules on hematoxylin and eosin are most likely these autolysosomal accumulations as suggested by their pattern of distribution and the fact that lysosomes are basophilic on H&E. Moreover, some clusters of autolysosomes are surrounded by membranes with sarcolemmal features but others are not. In support of this notion, ultrastructural studies identified 2 types of autophagic vacuoles: 1) clusters of autophagic vacuoles not surrounded by membranes or basal lamina, and 2) vacuoles containing various

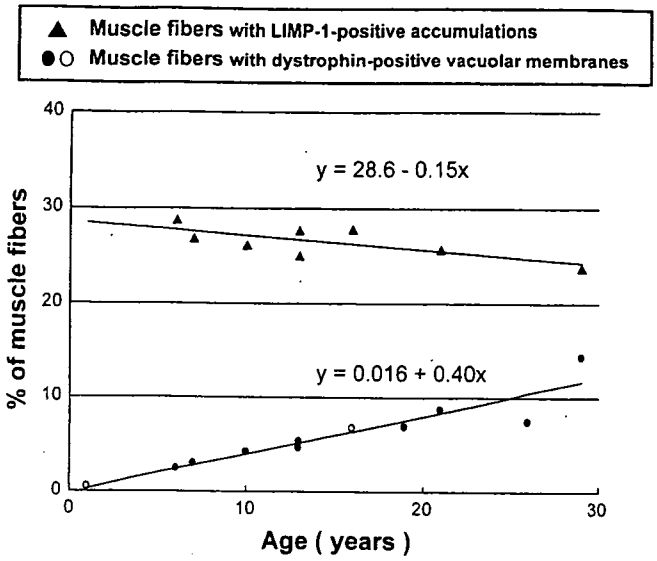

FIGURE 3. Relationship between age of the patients with Danon disease and number of muscle fibers with vacuoles highlighted with dystrophin or LIMP-1 on immunohistochemistry. The open circles show the only patient who had 2 muscle biopsies. The muscle fibers (circles) with intracytoplasmic vacuoles surrounded by dystrophin immuno-positive membrane (AVSFs) increased with age (r = 0.936). The muscle fibers (triangles) with overexpression of LIMP-1 showed a slight decrease with age (r = 0.353). r, Pearson's linear correlation coefficient.

autophagic materials encircled by membranes with basal lamina along the luminal side.

The proportion of muscle fibers with AVSFs increased with age in Danon disease and LAMP-2-deficient mice. In contrast, muscle fibers with LIMP-1-positive autolysosomal accumulations existed even in young patients and decreased slightly with age. It is most likely that the formation of these autolysosomal accumulations, which are clusters of autophagic vacuoles seen on electron microscopy, is a primary change in muscle fibers of Danon disease and related AVMs. The formation of peculiar membranes with sarcolemmal features around the autophagic vacuoles is hence a secondary phenomenon. Since muscle symptoms progress slowly in Danon disease, the development of muscle symptoms might be associated more closely with the formation of the unusual autophagic vacuoles rather than directly with the deficiency of LAMP-2.

LAMP-1 is the autosomal paralogous counterpart of LAMP-2 and both are thought to protect lysosomal membrane and cytoplasm from proteolytic enzymes within the lysosomes. LAMP-2 is tissue-specific but unlike LAMP 1, which is ubiquitously expressed, its expression is likely to be specifically regulated (26). Inhibition of LAMP-1 function results in failure of fusion of lysosomal and plasma membranes and therefore impaired exocytosis (27), a process usually by which cytoplasmic debris in the autophagosomes are extruded out from the cell through the sarcolemma (28). We therefore assume that LAMP-2 deficiency might likewise be related to dysregulation of exocytosis, leading to the development of the

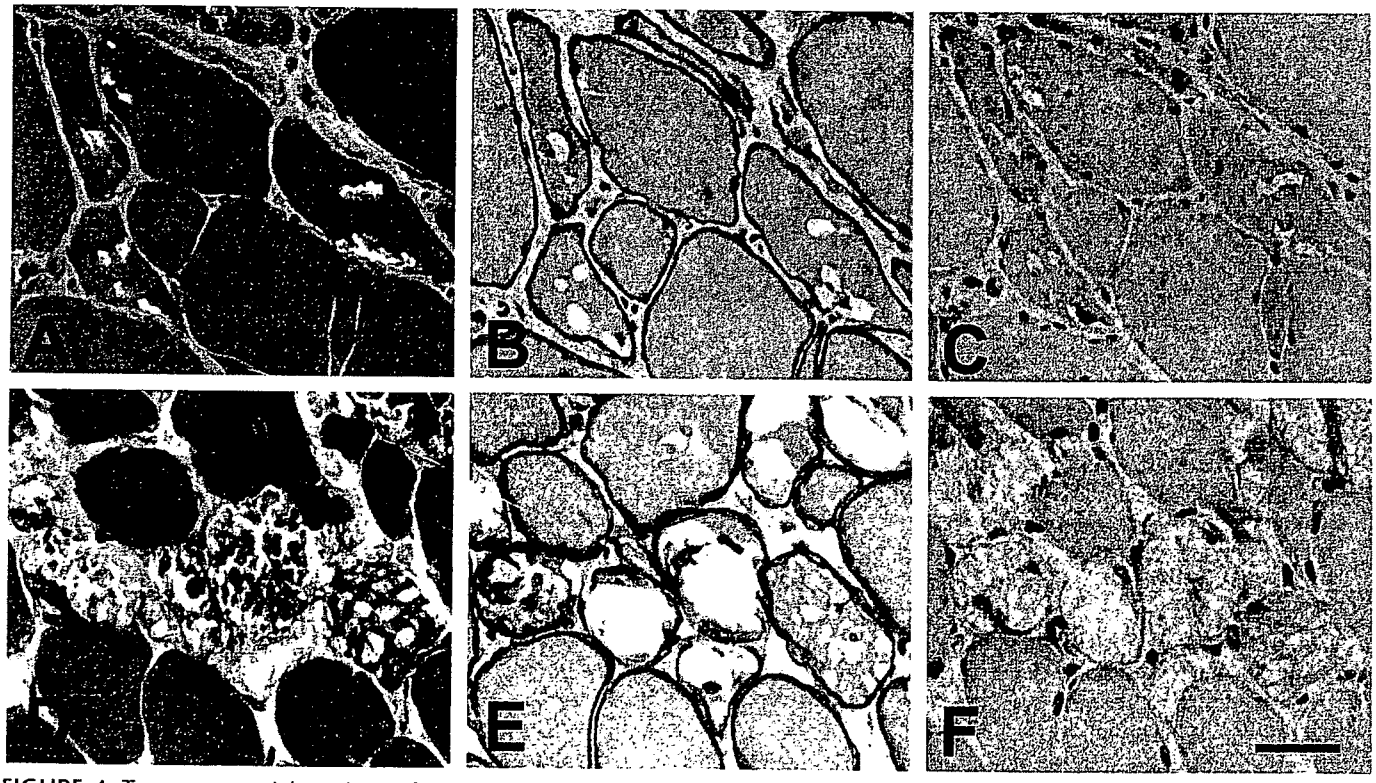

FIGURE 4. Transverse serial sections of muscle of patient with DMRV/HIBM (A–C) and with childhood AMD (D–F). Only a few rimmed vacuoles in DMRV/HIBM showed presence of dystrophin. In AMD, dystrophin is present on some vacuolar materials. However, no vacuolar membranes have AChE activity in DMRV/HIBM and AMD. (A, D): Gomori-trichrome stain; (B, E): AChE stain; (C, F): immunohistochemistry against dystrophin with DAB. Scale bar = 30 μm.

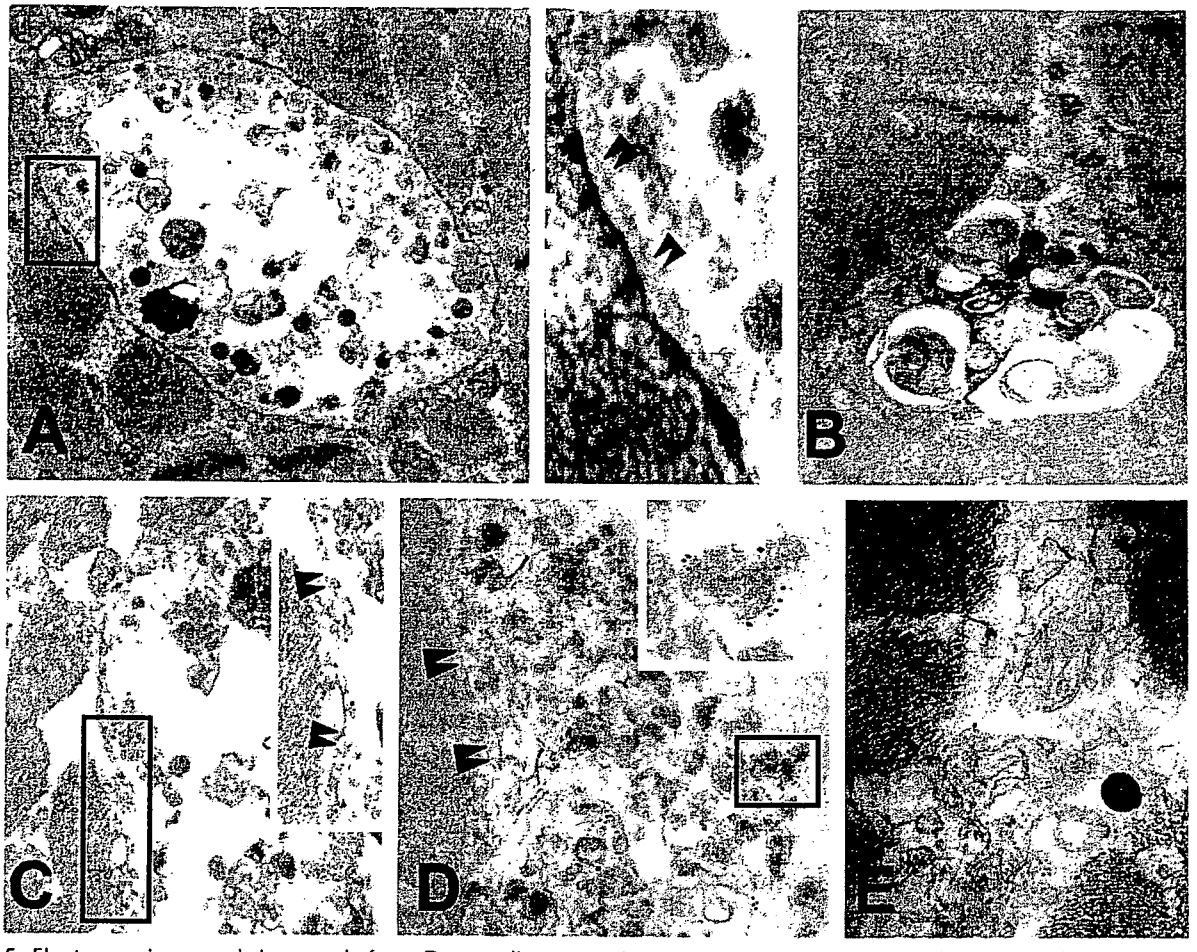

FIGURE 5. Electron micrograph in muscle from Danon disease patient. Scattered in the muscle fibers were clusters of autophagic vacuoles (A) containing cytoplasmic debris, electron dense material, and myeloid bodies. Some of these clusters were encircled by a membrane with basal lamina (paired arrowheads) on its luminal side, while other clusters are not limited by a membrane (B). Electron immunohistochemistry after single labeling with dystrophin or LIMP-1 antibody shows localization of the proteins in autophagic vacuoles (C–E). In the clusters with membranes, that is, the AVSF (A), the immunogold particles show dystrophin (C) along the vacuolar membrane (paired arrowheads), and the immunogold particles show LIMP-1 (D) around autophagic material inside autophagic vacuoles. In contrast, in the clusters not surrounded by membranes, immunogold particles show LIMP-1 around autophagic materials with absence of dystrophin (E). Original magnifications: (A) 15,000×; (B) 18,000×; (C) 20,000×; (D) 18,000×; (E) 30,000×.

unusual autophagic vacuoles with unique sarcolemmal features.

TfR and LDL-R are found in the membranes of recycling endosomes. In contrast, Rab5 and VAMP-7 are present in the membranes of early and late endosomes (29). We revealed the presence of all of these proteins in the fibers with autophagic vacuoles, indicating that in addition to the lysosomal system, the endosomal system is activated in Danon disease and related AVMs. Interestingly, VAMP-7 was increased in nonvacuolated fibers without autolysosomal accumulations, suggesting that maturation to late endosomes could prevent the formation of the unique vacuolar membranes.

Most of the vacuolar membranes were closed and were not connected to the sarcolemma in Danon disease. The autolysosomes containing cytoplasmic debris are therefore seen to be entrapped within the lumen of the vacuoles, and as such can be possibly considered to be extracellular space. Together with the observations that most AVSF did not accumulate in the subsarcolemmal region but were scattered in the cytoplasm, our findings suggest that the unique vacuolar membranes may be formed in situ in cytoplasm by a mechanism other than indentation of sarcolemma. One hypothesis is that the vacuolar membrane with basal lamina might be produced around clusters of autolysosomes (Fig. 6). The membranes surrounding the autophagic vacuoles might have originated from the lysosomal membrane or the isolation membrane that elongates and develops into the membrane of autophagosome (30), or is formed in situ and entirely de novo. If the vacuolar membranes are formed within the muscle fibers, it is compatible with the observation that the vacuolar membranes lack collagens IV and VI because collagens are thought to be produced mainly in the interstitium. Further studies are still necessary to understand the mechanism of the formation of these peculiar vacuolar membranes.

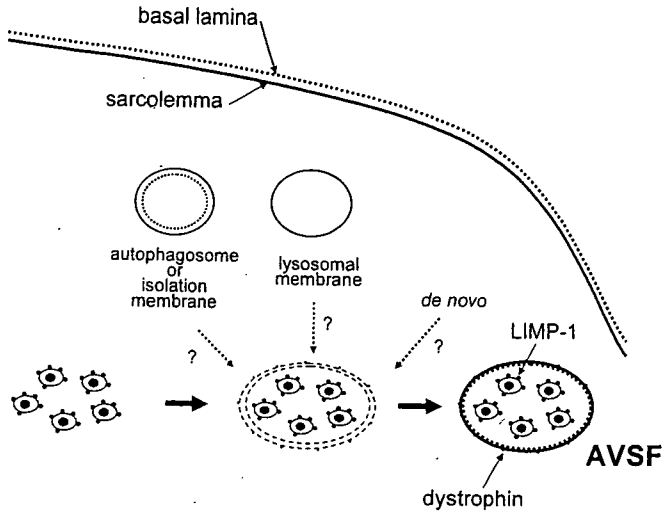

FIGURE 6. Schematic diagram of autophagic vacuoles in muscle fiber of patients with Danon disease. The membranes of the AVSFs were closed and were not connected to the sarcolemma. We suggest that the unique vacuolar membranes may be formed in situ in cytoplasm by a mechanism. One hypothesis is that the vacuolar membrane with basal lamina might be produced around clusters of autolysosomes, as illustrated.

In XMEA, vacuolar membranes have not been reported to have AChE activity (6). However, the strong similarity of the pathologic characteristics to Danon disease naturally raised the question of whether AChE activity is present in the vacuolar membranes in XMEA. Indeed, our Japanese patient with probable XMEA showed AChE activity in the vacuolar membranes. Therefore, Danon disease, XMEA, infantile AVM, and adult-onset AVM with multiorgan involvement share a common pathologic feature, namely, AVSF with AChE activity in the vacuolar membranes. Nevertheless, XMEA, infantile AVM, and adult-onset AVM are genetically different from Danon disease, as indicated by the presence of LAMP-2, which is absent in Danon disease. The observation that some features are not seen in Danon disease, like the presence of multilayered basal lamina and the deposition of C5b-9 over the surface of the muscle fiber, raise a possibility that some of these diseases might be allelic to XMEA, albeit different clinical phenotypes.

The autophagic vacuoles in AMD and rimmed vacuoles were reported to occasionally show presence of dystrophin. Nevertheless, these vacuoles are distinct from the AVSF seen in Danon disease and related AVMs, because the frequency of the vacuoles with sarcolemmal features is much less and most of sarcolemmal proteins are not consistently present in the vacuolar membranes of AMD and the rimmed vacuolar myopathies. Moreover, the activities of AChE and NSE were never found in the vacuolar membranes of these myopathies. In addition, on electron microscopy, the vacuolar membranes with basal lamina, such as those seen in Danon disease and related AVMs, were not found in AMD, DMRV/HIBM, or SIBM. According to the classification of De Bleecker et al, the AVSF may belong to type 1 vacuoles as the boundaries of type 1 vacuoles reacted for laminin, β-spectrin, and dystrophin (31). However, type 1 vacuoles were thought to be open to extracellular space and arise from invagination of the sarcolemma. Moreover, the membranes of AVSF have not only many sarcolemmal and extracellular proteins but also AChE activity, and may be formed in situ in cytoplasm as described above. Therefore, we think that the AVSF are a new, highly specific subtype of type 1 vacuoles.

Although the mechanism of their production still remains a mystery, overall, AVSF with AChE activity delineate Danon disease, XMEA, infantile AVM, and adult-onset AVM with multiorgan involvement from other AVMs. Most likely, this unique pathologic finding will probably be found in more diseases and therefore the list of AVMs in this group is likely to expand.

ACKNOWLEDGMENTS

The authors thank Drs. Shuzo M. Sumi (University of Washington, Seattle, WA) and May Christine V. Malicdan (NCNP, Tokyo, Japan) for their reviewing the manuscript. We also thank Dr. Michihiro Imamura (NCNP, Tokyo, Japan) for rabbit polyclonal anti-dystrophin antibody, Dr. Thierry Galli (Institut du Fer-à-Moulin, Paris, France) for mouse monoclonal anti-VAMP-7 antibody, Dr. Janice E. Sugiyama (National Institutes of Health, Bethesda, MD) for rabbit polyclonal anti-agrin antibody, and Dr. Yoshitaka Tanaka (Kyushu University, Fukuoka, Japan) for mouse monoclonal anti-LIMP-2 antibody. The authors thank Ms. Rika Oketa, Chiharu Yoshioka, and Fumie Uematsu (NCNP, Tokyo, Japan) for their technical assistance.

REFERENCES

1. Nishino I, Fu J, Tanji K, et al. Primary LAMP-2 deficiency causes X-linked vacuolar cardiomyopathy and myopathy (Danon disease). Nature 2000;406:906–10
2. Danon MJ, Oh SJ, DiMauro S, et al. Lysosomal glycogen storage disease with normal acid maltase. Neurology 1981;31:51–57
3. Sugie K, Yamamoto A, Murayama K, et al. The clinicopathological features of genetically confirmed Danon disease. Neurology 2002;58: 1773–78
4. Nishino I, Yamamoto A, Sugie K, Nonaka I, Hirano M. Danon disease and related disorders. Acta Myologica 2001;20:120–24
5. Murakami N, Goto Y, Itoh M, et al. Sarcolemmal indentation in cardiomyopathy with mental retardation and vacuolar myopathy. Neuromuscul Disord 1995;5:149–55
6. Kalimo H, Savontaus ML, Lang H, et al. X-linked myopathy with excessive autophagy: A new hereditary muscle disease. Ann Neurol 1988;23: 258–65
7. Yamamoto A, Morisawa Y, Verloes A, et al. Infantile autophagic vacuolar myopathy is distinct from Danon disease. Neurology 2001;57:903–5
8. Kaneda D, Sugie K, Yamamoto A, et al. A novel form of autophagic vacuolar myopathy with late-onset and multiorgan involvement. Neurology 2003;61:128–31
9. Nishino I. Autophagic vacuolar myopathies. Curr Neurol Neurosci Rep 2003;3:64–69
10. Tanaka Y, Guhde G, Suter A, et al. Accumulation of autophagic vacuoles and cardiomyopathy in LAMP-2-deficient mice. Nature 2000;406: 902–6
11. Saftig P, Tanaka Y, Lullmann-Rauch R, von Figura K. Disease model: LAMP-2 enlightens Danon disease. Trends Mol Med 2001;7:37–39
12. Sugie K, Koori T, Yamamoto A, et al. Characterization of Danon disease in a male patient and his affected mother. Neuromuscul Disord 2003;13: 708–11
13. Nishino I, Noguchi S, Murayama K, et al. Distal myopathy with rimmed vacuoles is allelic to hereditary inclusion body myopathy. Neurology 2002;59:1689–93

14. Takemitsu M, Nonaka I, Sugita H. Dystrophin-related protein in skeletal muscles in neuromuscular disorders:. Immunohistochemical study. Acta Neuropathol 1993;85:256–59
15. Metzinger L, Blake DJ, Squier MV, et al. Dystrobrevin deficiency at the sarcolemma of patients with muscular dystrophy. Hum Mol Genet 1997;6:1185–91
16. Ozawa E, Nishino I, Nonaka I. Sarcolemmopathy: Muscular dystrophies with cell membrane defects. Brain Pathol 2001;11:218–30
17. Tinsley JM, Blake DJ, Roche A, et al. Primary structure of dystrophin-related protein. Nature 1992;360:591–93
18. Collo G, Starr L, Quaranta V. A new isoform of the laminin receptor integrin α7β1 is developmentally regulated in skeletal muscle. J Biol Chem 1993;268:19019–24
19. Minetti C, Sotgia F, Bruno C, et al. Mutations in the caveolin-3 gene cause autosomal dominant limb-girdle muscular dystrophy. Nat Genet 1998;18: 365–68
20. Matsuda C, Aoki M, Hayashi YK, Ho MF, Arahata K, Brown RH Jr. Dysferlin is a surface membrane-associated protein that is absent in Miyoshi myopathy. Neurology 1999;53:1119–22
21. Kuo HJ, Maslen CL, Keene DR, Glanville RW. Type VI collagen anchors endothelial basement membranes by interacting with type IV collagen. J Biol Chem 1997;272:26522–29
22. Matthews-Bellinger JA, Salpeter MM. Fine structural distribution of acetylcholine receptors at developing mouse neuromuscular junctions. J Neurosci 1983;3:644–57
23. Ishikawa Y, Shimada Y. Acetylcholine receptors and cholinesterase in developing chick skeletal muscle fibers. Brain Res 1982;281:187–97
24. Fukuda M. Biogenesis of the lysosomal membrane. Subcell Biochem 1994;22:199–230
25. Winchester BG. Lysosomal membrane proteins. Eur J Paediat Neurol 2001;5:11–19
26. Kannan K, Divers SG, Lurie AA, Chervenak R, Fukuda M, Holcombe RF. Cell surface expression of lysosome-associated membrane protein-2 (lamp2) and CD63 as markers of in vivo platelet activation in malignancy. Eur J Haematol 1995;55:145–51
27. Reddy A, Caler EV, Andrews NW. Plasma membrane repair is mediated by Ca(2+)-regulated exocytosis of lysosomes. Cell 2001;106:157–69
28. Engel AG. Acid maltase deficiency. In: Engel AG, Banqer BQ, eds. *Myology*, Vol. 2. New York, NY: McGraw-Hill, 1993:1533–53
29. Advani RJ, Yang B, Prekeris R, Lee KC, Klumperman J, Scheller RH. VAMP-7 mediates vesicular transport from endosomes to lysosomes. J Cell Biol 1999;146:765–76
30. Mizushima N, Yamamoto A, Hatano M, et al. Dissection of autophagosome formation using Apg5-deficient mouse embryonic stem cells. J Cell Biol 2001;152:657–67
31. De Bleecker JL, Engel AG, Winkelmann JC. Localization of dystrophin and β-spectrin in vacuolar myopathies. Am J Pathol 1993;143:1200–1208
32. Sugiyama JE, Glass DJ, Yancopoulos GD, Hall ZW. Laminin-induced acetylcholine receptor clustering: An alternative pathway. J Cell Biol 1997;139:181–91

Centronuclear myopathy in mice lacking a novel muscle-specific protein kinase transcriptionally regulated by MEF2

Osamu Nakagawa,[1,8] Michael Arnold,[1] Masayo Nakagawa,[1] Hideaki Hamada,[1] John M. Shelton,[2] Hajime Kusano,[4] Thomas M. Harris,[5] Geoffrey Childs,[5] Kevin P. Campbell,[4] James A. Richardson,[1,3] Ichizo Nishino,[6] and Eric N. Olson[1,7]

[1]Department of Molecular Biology, [2]Department of Internal Medicine, and [3]Department of Pathology, The University of Texas Southwestern Medical Center at Dallas, Dallas, Texas 75390, USA; [4]Howard Hughes Medical Institute and Department of Physiology and Biophysics, The University of Iowa Roy J. and Lucille A. Carver College of Medicine, Iowa City, Iowa 52242, USA; [5]Department of Molecular Genetics, Albert Einstein College of Medicine, Bronx, New York 10461, USA; [6]Department of Neuromuscular Research, National Institute of Neuroscience, National Center of Neurology and Psychiatry, Tokyo 187-8502, Japan

Myocyte enhancer factor 2 (MEF2) plays essential roles in transcriptional control of muscle development. However, signaling pathways acting downstream of MEF2 are largely unknown. Here, we performed a microarray analysis using *Mef2c*-null mouse embryos and identified a novel MEF2-regulated gene encoding a muscle-specific protein kinase, Srpk3, belonging to the serine arginine protein kinase (SRPK) family, which phosphorylates serine/arginine repeat-containing proteins. The *Srpk3* gene is specifically expressed in the heart and skeletal muscle from embryogenesis to adulthood and is controlled by a muscle-specific enhancer directly regulated by MEF2. *Srpk3*-null mice display a new entity of type 2 fiber-specific myopathy with a marked increase in centrally placed nuclei; while transgenic mice overexpressing *Srpk3* in skeletal muscle show severe myofiber degeneration and early lethality. We conclude that normal muscle growth and homeostasis require MEF2-dependent signaling by Srpk3.

[*Keywords*: Myocyte enhancer factor 2; transcriptional regulation; serine arginine protein kinase (SRPK); Stk23/Srpk3; centronuclear myopathy]

Supplemental material is available at http://www.genesdev.org.

Received May 31, 2005; revised version accepted July 7, 2005.

Skeletal muscle differentiation is cooperatively controlled by two families of transcription factors, the myogenic basic helix–loop–helix (bHLH) proteins and the myocyte enhancer factor 2 (MEF2) family of MADS domain proteins (Black and Olson 1998; Bailey et al. 2001; Pownall et al. 2002; Buckingham et al. 2003; Parker et al. 2003). Myogenic bHLH proteins, such as MyoD and myogenin, recognize a DNA sequence called an E box (CANNTG). Myogenic bHLH proteins associate and synergistically activate transcription with MEF2 factors, which bind to the A/T-rich DNA consensus (CTA-(A/T)$_4$-TA-G/A). Additionally, myogenic bHLH proteins activate their own expression and the expression of MEF2, while MEF2 stimulates expression of myogenic bHLH protein genes and the *Mef2c* gene (Cserjesi and Olson 1991; Lassar et al. 1991; Edmondson et al. 1992; Cheng et al. 1993; Yee and Rigby 1993; Wang et al. 2001; Teboul et al. 2002; Dodou et al. 2003). Such auto- and cross-regulatory interactions establish a mutually reinforcing circuit to achieve myogenesis.

The essential role of MEF2 in muscle development was first shown in *Drosophila* in which a loss-of-function mutation in the single MEF2 ortholog *D-mef2* results in a complete block to differentiation of all muscle lineages: somatic, cardiac, and visceral (Bour et al. 1995; Lilly et al. 1995). In mice, the existence of four *Mef2* genes—*Mef2a*, *Mef2b*, *Mef2c*, and *Mef2d*—with overlapping expression patterns makes it more difficult to assess the roles of these factors individually (Black and Olson 1998). Mice homozygous for a *Mef2c*-null allele show embryonic lethality around embryonic day 9.5 (E9.5) caused by improper development of the heart (Lin et al. 1997). The mutant hearts do not undergo looping morphogenesis, the future right ventricle does not form, and

Corresponding authors.
[7]**E-MAIL eric.olson@utsouthwestern.edu; FAX (214) 648-1196.**
[8]**E-MAIL osamu.nakagawa@utsouthwestern.edu; FAX (214) 648-1450.**
Article and publication are at http://www.genesdev.org/cgi/doi/10.1101/gad.1338705.

a subset of cardiac muscle genes is not expressed. MEF2 has also been implicated in maintenance of the slow fiber phenotype of skeletal muscle, in the control of striated muscle energy metabolism, and in pathological remodeling of the adult heart in response to stress signaling (Black and Olson 1998; McKinsey et al. 2002).

In principle, MEF2 may regulate muscle-specific target genes directly, or it may act indirectly by controlling the expression of subordinate transcription factors or signaling molecules that act as intermediaries to connect MEF2 to downstream targets that themselves are not dependent on MEF2-binding sites in their *cis*-regulatory regions. Indeed, vast arrays of direct and indirect targets of MEF2 in skeletal muscle cells in culture were recently described (Blais et al. 2005).

In an effort to identify MEF2 target genes that serve as "downstream" effectors of MEF2 action during muscle development, we performed a microarray analysis using *Mef2c*-null embryos and identified a novel muscle-specific protein kinase Stk23/Srpk3, which is encoded by a direct MEF2 target gene. *Srpk3*-null mice display a new entity of centronuclear myopathy, while transgenic mice overexpressing *Srpk3* in skeletal muscle show severe myofiber degeneration. These findings reveal an essential role for serine arginine protein kinase (SRPK)-mediated signaling in muscle growth and homeostasis downstream of MEF2 transcription factors.

Results

Srpk3: *a novel muscle-specific protein kinase gene*

In an attempt to identify novel MEF2-regulated genes, we compared the gene expression profiles of hearts from wild-type and *Mef2c*-null mouse embryos by an RNA microarray analysis. Because *Mef2c*-null embryos die around E9.5 (Lin et al. 1997), we used hearts from wild-type and null embryos at E9.0 prior to overt cardiac demise. Among the genes that were dysregulated in the *Mef2c* mutants, we found the expression of *Stk23* to be significantly decreased in the *Mef2c*-null hearts. The down-regulation of *Stk23* expression in the *Mef2c*-null hearts was confirmed by RT–PCR (Fig. 1a). Residual expression of *Stk23* in the mutants may reflect the presence of other MEF2 factors that partially compensate for MEF2C.

Stk23 was described in an analysis of human chromosomal DNA methylation as a potential protein-kinase-encoding gene (Grunau et al. 2000), but its expression profile and function have not been described. Structural comparison with various protein kinases clearly indicated that Stk23 possesses a bipartite kinase domain with high sequence similarity to the SRPK family kinases, Srpk1 and Srpk2 (Fig. 1b,c; Gui et al. 1994; Bedford et al. 1997; Kuroyanagi et al. 1998; Wang et al. 1998). As expected, Stk23 efficiently phosphorylated known SRPK

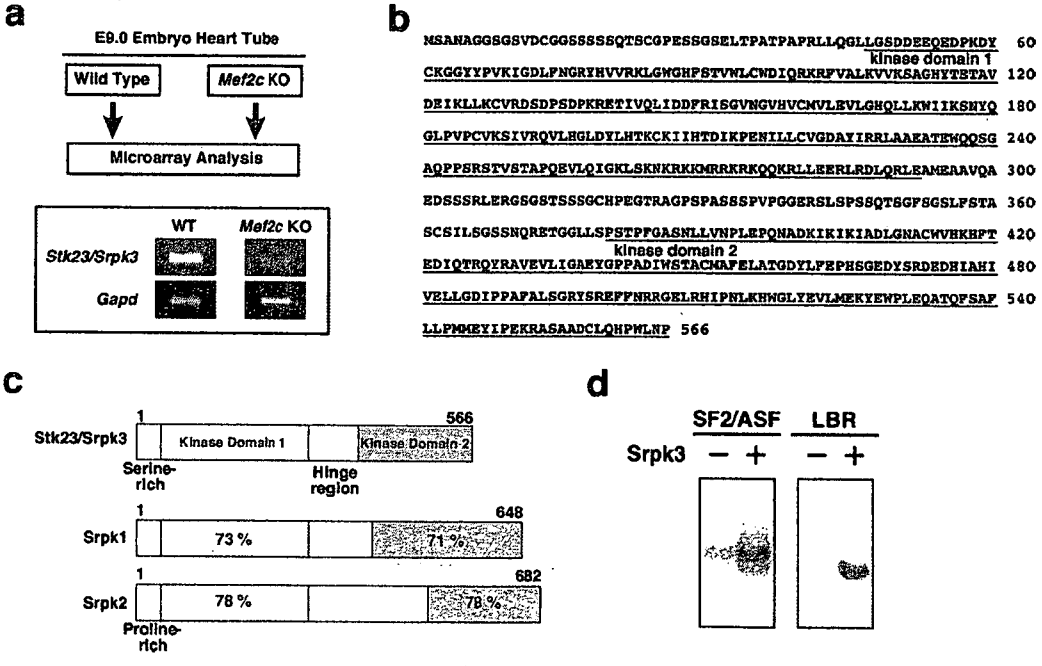

Figure 1. Identification of Stk23/Srpk3 as a novel SRPK. (*a*) Microarray analysis was performed using the hearts of E9.0 *Mef2c*-null and wild-type embryos. Down-regulation of the *Stk23/Srpk3* expression in the *Mef2c*-null hearts was confirmed by RT–PCR. (*Gapd*) Glyceraldehyde-3-phosphate dehydrogenase expression as a control. (*b*) Amino acid structure of mouse Stk23/Srpk3. Srpk3 is a 566-amino-acid protein that contains a bipartite kinase domain (underlined), N terminus, and a hinge region. (*c*) Schematic representation of mouse SRPK family kinases. Srpk3 shows high sequence similarity to Srpk1 and Srpk2 in the kinase domain, but not in the N terminus and hinge region. The percentages in the boxes are identities of Srpk1 and Srpk2 to Srpk3 at an amino acid level. Srpk3 and Srpk2 have serine- and proline-rich sequences in the N terminus, respectively. Amino acid numbers are also shown. (*d*) Phosphorylation assays using SR domain proteins. Srpk3 phosphorylated SF2/ASF and the N-terminal region of Lamin B Receptor (LBR) in vitro.

substrates, the splicing factor SF2/ASF, and Lamin B Receptor in in vitro kinase assays (Fig. 1d; Nikolakaki et al. 1997; Koizumi et al. 1999; Yeakley et al. 1999; Takano et al. 2002). Therefore, we propose a functionally descriptive nomenclature, Srpk3, for Stk23.

In situ hybridization with mouse embryos showed *Srpk3* to be specifically expressed in the developing heart, somites, and skeletal muscles, in contrast to broad expression of Srpk1 and Srpk2 (Fig. 2a). Expression in the heart was first detected in the heart tube, immediately following expression of MEF2C, and expression in the somite myotomes was observed by E9.5. Within the embryonic heart, *Srpk3* is expressed throughout the atrial and ventricular chambers (Fig. 2a). *Srpk3* is highly expressed in the heart and skeletal muscle in adult mice (Fig. 2b). Muscle-specific expression was also observed in human fetal and adult tissues (Supplementary Fig. 1).

Regulation of the Srpk3 promoter by MEF2

To examine if *Srpk3* is transcriptionally regulated by MEF2, we performed reporter analyses in vitro and in vivo. MEF2C and MyoD significantly activated the expression of a luciferase reporter controlled by a 2.9-kb DNA fragment encompassing the 5′ *Srpk3* promoter region, and serial deletion analysis revealed that a 0.4-kb fragment was sufficient for the activation by MEF2C and MyoD (Fig. 3a). Indeed, the 0.4-kb fragment contains a MEF2-binding site and two E boxes (Fig. 3b). Although there are also two GATA sites in the 0.4-kb fragment, GATA proteins did not enhance *Srpk3* promoter activity in luciferase assays (data not shown). An oligonucleotide probe, containing the MEF2 site and E boxes in the *Srpk3* promoter, was bound by MEF2C as well as by myogenin and its ubiquitous bHLH dimerization partner, E12 (Fig. 3c). Mutation of the MEF2 site in the context of the 2.9- or 0.4-kb fragment significantly decreased the response to MEF2C and MyoD in luciferase assays (Fig. 3d), suggesting that MEF2 is an obligate activator of the *Srpk3* promoter.

Transcriptional control of Srpk3 during myogenic differentiation in vitro

We next examined the expression of *Srpk3* mRNA during differentiation of C2C12 myoblasts, which are triggered to differentiate and form myotubes upon transfer to medium with low serum (Lu et al. 2000). *Srpk3* mRNA was not expressed in C2C12 myoblasts but was markedly induced together with embryonic and perinatal myosin genes, *Myh3* and *Myh8*, during myogenesis (Fig. 3e).

Consistently, expression of a luciferase reporter controlled by the *Srpk3* promoter was markedly enhanced during differentiation of C2C12 cells (Fig. 3f). Mutation of the MEF2 site almost abolished the promoter activity, suggesting that *Srpk3* expression is activated upon myogenic differentiation directly by MEF2 proteins.

Transcriptional control of Srpk3 in vivo

We further examined the transcriptional regulation of *Srpk3* expression in transgenic mice. The 2.9-kb and 0.4-kb *Srpk3* regulatory regions fused to the *HSP68* basal promoter (Fig. 4a) directed the expression of a *LacZ* reporter in the embryonic heart and somites (Fig. 4b,c), recapitulating the muscle-specific expression pattern of the endogenous gene. The 0.4-kb fragment was also sufficient to direct muscle-specific expression without the *HSP68* minimal promoter (data not shown). Analyses of embryo sections confirmed that *LacZ* expression was observed throughout cardiac muscle walls, including the outflow tract, and in the somite myotomes (data not shown).

Consistent with the luciferase reporter analyses, the mutation of the MEF2-binding site in the context of the 0.4-kb fragment completely abolished *LacZ* expression in the heart and somites. Ten out of 16 transgenic embryos harboring the transgene with the mutant MEF2 site showed no LacZ staining (Fig. 4d), and the remaining showed weak ectopic expression that was not specific to

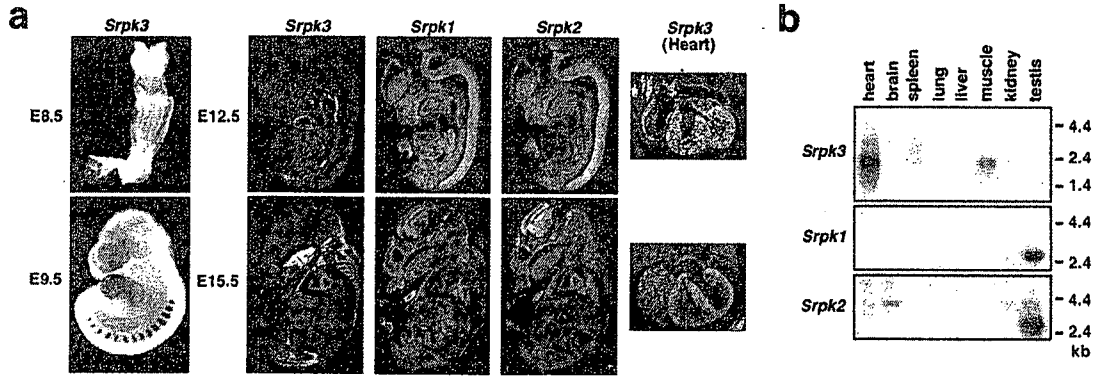

Figure 2. Muscle-specific expression of Srpk3. (*a*) Expression of the SRPK family in mouse embryos. Whole-mount and section in situ hybridization. *Srpk3* is expressed exclusively in the developing heart, somites, and embryonic skeletal muscle. *Srpk1* and *Srpk2* are widely expressed in embryonic tissues, with enrichment in the neural tube and brain. Enlargements of the heart from each stage are shown to the *right*. (*b*) Expression of the SRPK family in adult mice. *Srpk3* is specifically expressed in the heart and skeletal muscle, with a faint expression in the spleen. Testis-enriched expression of *Srpk1* and *Srpk2* is also shown *below*. With longer exposure, lower levels of *Srpk1/-2* expression were observed ubiquitously.

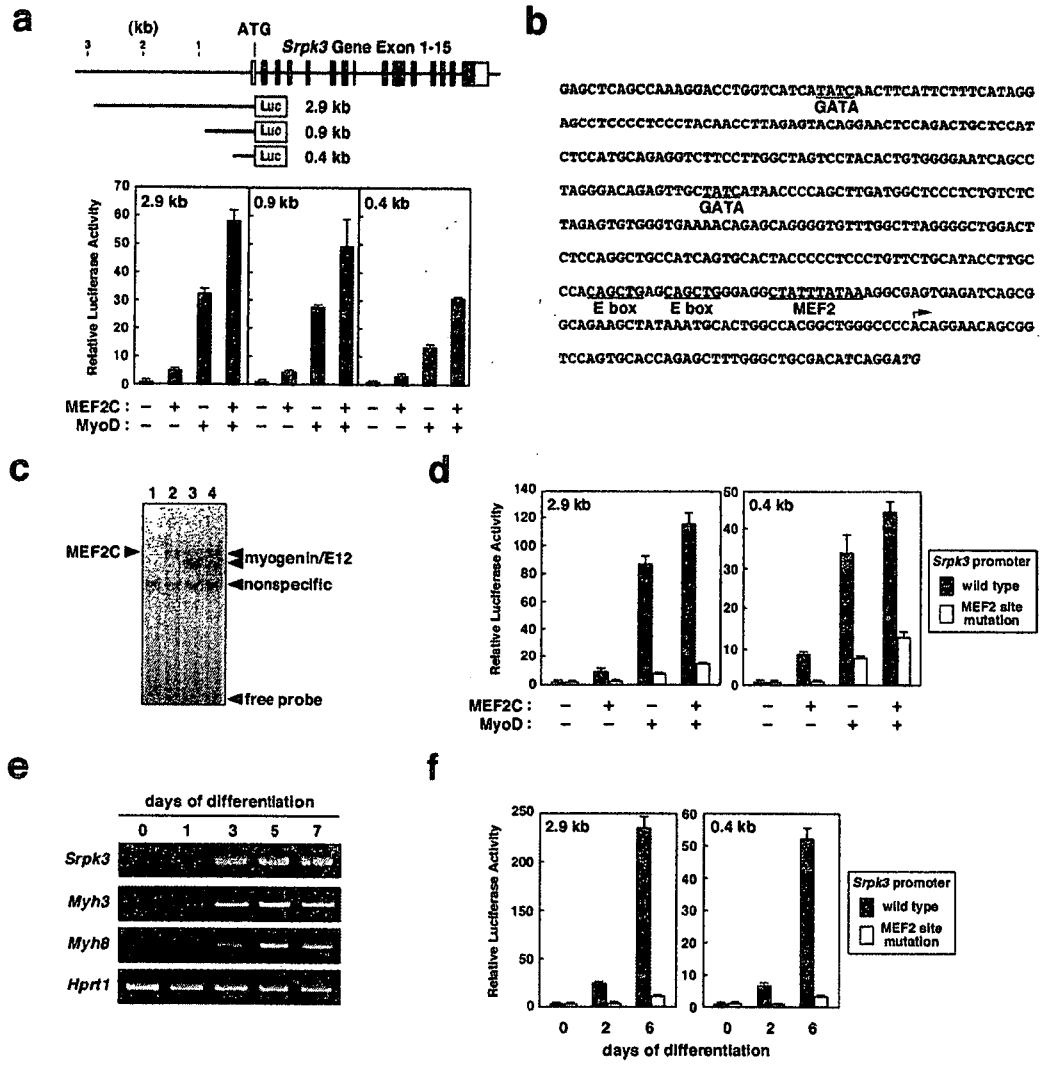

Figure 3. MEF2-dependent muscle-specific transcription of Srpk3. (*a*) The structure of the mouse *Srpk3* gene with schematics of the luciferase constructs and the results of luciferase assays are shown. Filled and open boxes indicate the exons for protein-coding and noncoding regions, respectively. MEF2C and MyoD strongly activate luciferase reporter expression controlled by the *Srpk3* enhancer/promoter in C2C12 myoblasts. The 0.4-kb fragment is sufficient for the response. (*b*) Sequence of the 0.4-kb minimal muscle enhancer/promoter of *Srpk3*. The MEF2-binding site, E boxes, and GATA-binding sites are underlined. The putative transcriptional start site estimated by the most 5′-end of Srpk3 cDNA clones is indicated by an arrow. The translational start site (*ATG*) is italicized. (*c*) MEF2C and the myogenin/E12 complex bind to the fragments encompassing the MEF2 site and E boxes in the minimal muscle enhancer of *Srpk3*. Electrophoretic mobility shift assay. (Lane *1*) Control. (Lane *2*) MEF2C. (Lane *3*) Myogenin and E12. (Lane *4*) MEF2C, myogenin, and E12. (*d*) Mutation of the MEF2-binding site in the context of the 2.9- or 0.4-kb *Srpk3* fragments significantly impairs the response to MEF2C and MyoD in luciferase assays. (*e*) *Srpk3* expression is activated by 1 d after stimulation during myogenic conversion of C2C12 cells. Expression patterns of embryonic and perinatal myosins, *Myh3* and *Myh8*, respectively, are also shown. (*Hprt1*) Hypoxanthine guanine phosphoribosyl transferase 1 as a control. (*f*) Activity of the *Srpk3* luciferase reporters is markedly stimulated during myogenic conversion of C2C12 cells, while mutation of the MEF2-binding site almost abolishes it.

the heart and somites. In contrast, mutation of the two E boxes did not result in a significant decrease of *LacZ* expression in the heart and somites (Fig. 4e). We conclude that *Srpk3* is a direct transcriptional target of MEF2 proteins in vivo.

Muscle defects in Srpk3 transgenic mice

SRPKs are known to regulate mRNA splicing and the assembly of nuclear lamina proteins, by phosphorylating SR splicing factors and Lamin B Receptor (Gui et al. 1994; Bedford et al. 1997; Nikolakaki et al. 1997; Kuroyanagi et al. 1998; Wang et al. 1998; Koizumi et al. 1999; Yeakley et al. 1999; Takano et al. 2002). RNAi experiments showed that SRPK is essential for germline development in *Caenorhabditis elegans* (Kuroyanagi et al. 2000), but in vivo functions of the SRPK family have not been examined in mammals.

To analyze the effects of excessive SRPK activity in striated muscles, we generated transgenic mice overex-